IASS 2018 BOSTON, JULY 16-20
CREATIVITY IN STRUCTURAL DESIGN

Proceedings of the IASS Annual Symposium 2018
Creativity in Structural Design
July 16-20, 2018, MIT, Boston, USA
Caitlin Mueller, Sigrid Adriaenssens (eds.)

High Fidelity Additive Manufacturing of Transparent Glass Structures

Chikara INAMURA[1], Michael STERN[1], Daniel LIZARDO[1], Peter HOUK[2], and Neri OXMAN[1*]

*neri@mit.edu
[1] MIT Media Lab, Massachusetts Institute of Technology, Cambridge, MA 02139
[2] MIT Glass Lab, Massachusetts Institute of Technology, Cambridge, MA 02139

Abstract:

Optically transparent and structurally sound, glass plays a significant role in the development of the built environment and its relationship with the natural environment. Glass manufacturing methods such as blowing, pressing, and forming–along with modern float glass processes–all aim to increase performance and functionality. Nonetheless, techniques and technologies enabling controlled tunability of optical and mechanical properties at high spatial resolution remain an end without a means. This paper presents novel design, engineering, and construction processes of large-scale 3D printed glass structures enabled by a new high-fidelity large-scale additive manufacturing technology for optically transparent glass. The described research builds upon previous work conducted by The Mediated Matter Group at MIT in scaling a proof-of-concept to an industrial manufacturing process. The present technology makes novel use of digitally integrated thermal control and motion control systems to produce glass structures with tunable and predictable mechanical and optical properties. Illustrative structures in the form of three-meter tall freestanding glass columns were optimized under material constraints of the viscoelastic filaments to provide highly efficient structural and optical performance. A motion-controlled light was integrated inside each column, and the interplay between light and changing morphology of the printed glass was optically magnified, transforming the exhibition space into a dynamic landscape of luminous caustics. A series of material and mechanical characterizations were conducted in order to evaluate the fidelity and repeatability of the new manufacturing platform, as well as the structural performance of the resulting glass products in order to determine the safety factors required to execute a public installation. The 3D printed glass structures presented here were exhibited for the first time at the Triennale Design Museum as part of Milan Design Week 2017.

Keywords: 3D Printing, Additive Manufacturing, Glass, Glass Structure, Glass Architecture, Transparency, Light, Caustics

1. Introduction

Glass was introduced in architecture around 100 ACE when it was used to glaze the first windows [1]. Glass making techniques evolved slowly and remained expensive through the next two millennia. The Crystal Palace by Joseph Paxton was built in 1851 for the Great Exhibition in London, manifesting a new possibility of glass in architecture with its fully transparent building envelop that covered over 70,000 square meters of floor area with 300,000 hand blown glass panels [2]. With the introduction of the industrial manufacturing process for float glass in 1959, the application of glass in architecture has continued to grow into a 45 billion dollar industry worldwide [3][4]. Representing 59 million tons or approximately 7.3 billion square meters of flat glass, this standardized production has achieved economy of scale and transformed the building landscape, mediating between our environment and our homes and workplaces with windows, roofs, and facades. Recent trends in architecture have given rise to complex forms, at times requiring large production of customized double curved panels. Standard glass manufacturing methods do not support effective mass customization deployed at either product

or architectural scales. As a result, a number of different research groups have embarked on the development of glass 3D printers as a means to fabricate complex custom objects.

2. The Platform Space: From Prototype to Industrial Platform

2.1. Additive Manufacturing of Glass

The second-generation molten glass printer G3DP2 was built upon research previously conducted in the Mediated Matter Group [5]. Development of G3DP2 focused on creating a system that could support the production of glass at an architectural scale [6]. This required increased speed, scale, repeatability, and reliability. These four objectives were used to measure the efficacy of the system in comparison to the previous prototype, G3DP, as well as to other glass additive manufacturing systems, specifically from the research by Kotz et al and the commercial work by Micron 3DP [7][8]. Key metrics are compared across these platforms in Table 1. This comparison highlights the critical speed and scale improvements that enable G3DP2 to accomplish the desired architectural output. Critically, the deposition rate of G3DP2 is 5.2 kg/hr, 260 times faster than the Kotz system and 104 times faster than the Micron 3DP system. This deposition rate is one of the fastest across all materials in additive manufacturing [9], and paired with large build volume, repeatability, and industrial reliability, G3DP2 is the first glass printer to achieve architectural production.

Table 1: Comparison of glass additive manufacturing platforms

Platform	*Unit*	*Kotz et al*	*Micron 3DP*	*G3DP*	*G3DP2*
Print Volume	*[L]*	*0.1*	*12.0*	*18.8*	*35.8*
Layer Height	*[mm]*	*0.020*	*0.1*	*4.5*	*5.0*
Print Rate	*[kg/hr]*	*0.02*	*0.05*	*2.2*	*5.2*

2.2. G3DP2

The G3DP2 platform is composed of a two-part modular assembly with a stationary, three-zone thermal control module and four-axis motion control module. These two systems are driven by a software interface that translates digital designs into physical glass objects. The software workflow developed for the printer consists of the following phases. The first is the design phase where the three-dimensional object is computationally modeled using the CAD software Rhinoceros 5.0 (Robert McNeel & Associates, Seattle, WA). During this stage, the design of an object is generated as a single continuous contour line that serves to define both its form and the machine path that will be used to fabricate it. The object is then translated with custom C# modules from a geometric path into an executable G-Code file. This file is loaded into a machine code executor, ChiliPeppr, which sends instructions to the motion control module through a CNC motion control hardware TinyG, which then sends commands to individual motors on the four axes X, Y, Z, and A-axis, which controls the rotation about the Z-axis. Critical to the repeatability and reliability of the system, onboard closed-loop servomotors ClearPath (Teknic, Inc., Victor, NY) were selected and coupled with high-precision linear actuators and rotary table.

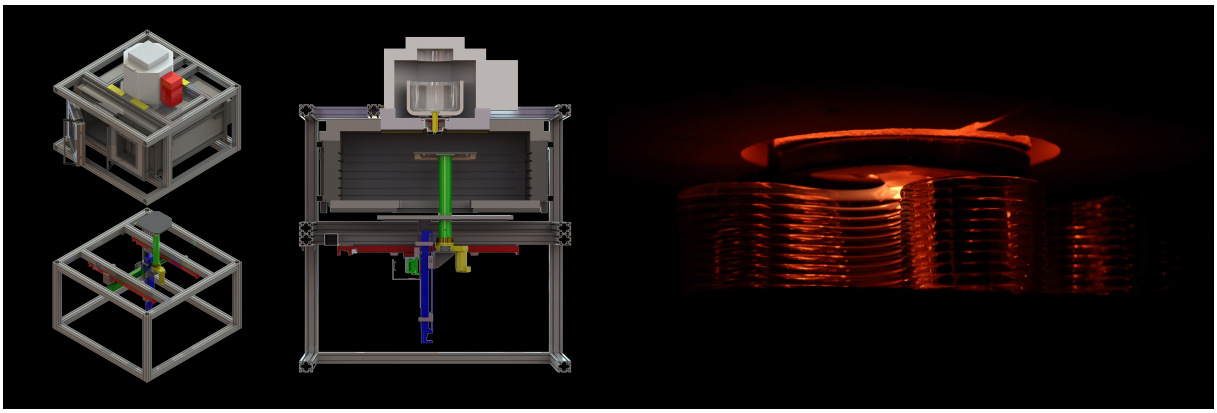

Figure 1: G3DP2 Platform (left) and deposition process (right)

The thermal control module consists of three independently controlled thermal regions that operate in concert to process the molten glass stock into a stress-free product. The material reservoir, where molten glass is stored, is kept at 1090 ºC. The glass flows down through the temperature-controlled nozzle, where it is conditioned at 915 ºC to set it at a desirable viscosity for printing. Finally, the glass is deposited into the build chamber, which is kept at 480 ºC, allowing for the glass to cool and stabilize as it is printed. The build chamber facilitates a stable temperature where the glass stops flowing while allowing it to relax its thermal stress, ensuring proper adhesion between layers and resulting in a stress-free glass product.

3. The Product Space: From Object to Structure

3.1. Structural Use of Glass

Structural use of glass in architecture is gaining momentum in both scale and diversity of applications, but its modality is largely limited to the use of float glass. Brittle fracture and the absence of a standard material strength sets glass apart from other building materials when it comes to structural applications. In order to compensate the lack of ductility in the material, composite glass structures are employed to increase the strain energy in the post fracture phase and improve overall safety. Laminated panels for facades, roofs, floors and staircases, as well as composite glass beams with adhesive bonded post-tensioned steel tendon are some novel examples of glass structures [10].

3.2. Strength of Glass

Glass is elastic and brittle. Its strength depends on the size and distribution of the inherent mechanical flaws within the material. As glass scales in volume, so does the average size and number of internal flaws. These flaws concentrate stress, and unlike in ductile materials capable of relaxing that stress, the dense but amorphous structure of glass prevents internal strain and leads to brittle fracture. The tensile strength of glass is inversely proportional to the size of the internal flaws in logarithmic scale. Inhomogeneity in the size and density of the flaws increases proportionally to the scale of the glass object, leading to wider scattering of the overall strength. Manufacturing processes introduce additional surface flaws through mechanical contact and abrasion. Architectural scale applications requiring flexure strength are particularly sensitive to surface flaws as overall strength is bound by the tensile stress on its exterior surface. Statistical approaches have been developed to standardize the expected strength of each glass product as a function of the probability of failure. Typically, material scale laboratory testing is conducted, and the Weibull distribution function is applied to the acquired data to model a continuous function of strength based on the probability of failure. Nominal strength and distribution shape varies across products based on the manufacturing processes. A tensile strength of 45 MPa at 5% probability of failure is often reported for a standard soda-lime glass sheet produced by a float glass process [11].

3.3. Glass Column

G3DP2 was developed to produce industrial-grade glass products for structural and architectural applications. In order to evaluate the manufacturing processes and demonstrate its capability, a series of large-scale structural columns was printed. Each column was designed as a three-meter tall freestanding and post-tensioned structure with continuously varying cross-sections that were assembled with a series of 3D printed glass products. In parallel, a series of laboratory tests were conducted on selected glass products to evaluate the mechanical properties and responses of the printed glass under various loading conditions. Numerical analysis was conducted on selected samples based on the results from the laboratory tests to further examine the stress distribution and critical stress leading to the ultimate failure of the relatively thick-wall cylindrical glass structures under axial compression. The following sections present the design, engineering, fabrication, and construction processes of the installation along with the summary of the mechanical characterizations.

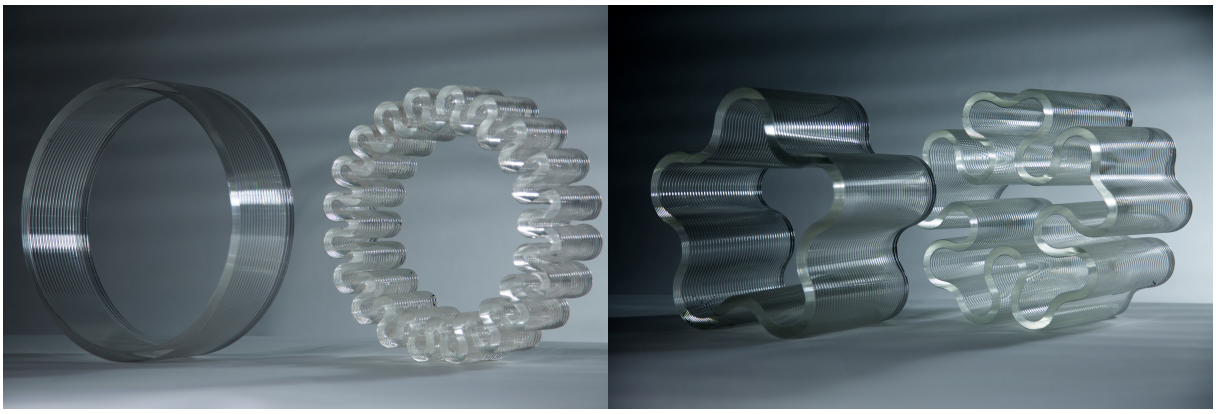

Figure 2: Constant curvature based design morphology of the 3D printed glass products: showing the range of curvatures (left), and morphology of the five-petal glass column (right)

3.4 Computational Design

The viscoelastic nature of molten glass and the deposition of large-diameter filament presents a unique design space where process fidelity is influenced by curvature of the print geometry and the resulting dynamic shear force exerted on the glass filament during its deposition. In general, the higher the curvature, the greater the shear force during deposition, leading to larger deviation of the output. Especially for structural applications, brittleness of the material leaves very little room for deviations in curvature, as they can become a source of stress concentration and lead to fracture. Based on these observations, a suite of computational design tools was developed, where an explicit control of curvature was defined as an input variable. A curvature based parametric design space for the glass columns was established based on a radial array of constant radius arcs and interconnecting bi-tangent arcs. Geometrical properties such as section area, section modulus, and area moment of inertia, were calculated in real-time to provide feedback and facilitate an intuitive workflow for navigating the design space, enabling optimization of structural performance. For the freestanding cantilever columns, design configurations were optimized such that higher section modulus and area moment of inertia occurred at the bottoms of the columns while minimizing mass. Based on this, three unique configurations of glass columns were designed and produced. Figure 3 presents the diagram of the cross-section profiles along with the isometric views of each configuration.

3.5. Engineering

Each glass column was assembled from fifteen glass products manufactured by the G3DP2 platform. Each product was unique in shape but shared a standard cylindrical bounding size of 300 mm in diameter by 200 mm in height, resulting in an overall column height of 3000 mm. The top and bottom faces were ground flat and polished prior to assembly to ensure planarity. In order to prevent stress concentration at contact interfaces, a thin layer of transparent silicon with compressive strength of 3MPa (2K Silicone Verifix, Bohle Ltd., Cheshire, UK) was applied to the bottom face of each glass product. The silicone was cured before assembly to form a dry joint that facilitated on-site assembly and disassembly for maintenance and transportation. To encourage monolithic behavior and ensure flexural strength against lateral load, each glass column was post-tensioned by a steel member through the central axis and anchored to steel plates at both ends. To ensure safety for visitors, the designed lateral load for the glass columns was determined based on the European structural standard for horizontal load on a residential handrail (BS EN 1991-1-1) as a concentrated load of 0.25kN at 1.0m in height from the ground. Minimum pre-stress value was determined as 4.5kN based on the bending moment induced by the designed lateral load such that equivalent tensile stress is properly canceled by the pre-stress. The base plate was designed to provide necessary counter weight and to extend the moment arm in order to prevent overturn against the lateral load.

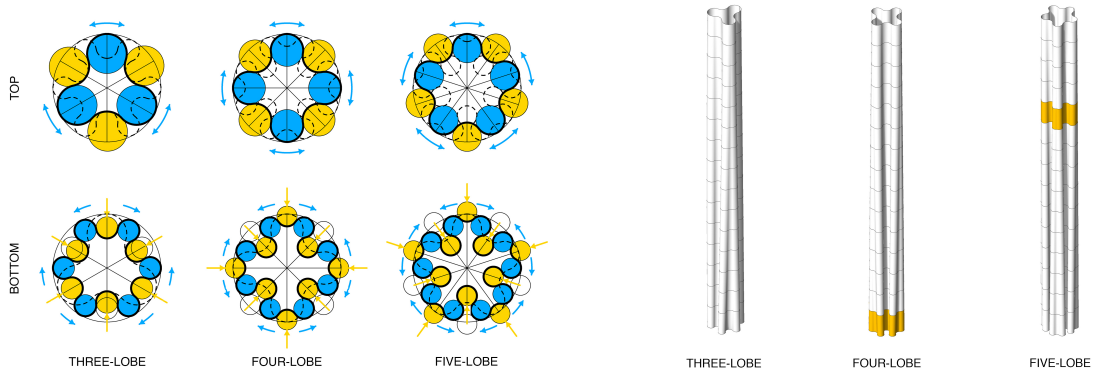

Figure 3: Design of the glass columns: section diagram with underlining convex arcs in blue and concave arcs in yellow (left), and isometric view with components highlighted in yellow (right)

3.6. Installation

Including a full-scale backup for one of the columns, a total of four sets of three-meter tall glass columns were prepared, resulting in production of 60 custom designed 3D printed glass products. Individual product mass ranged from 5 kg to 10 kg based on morphology, for a total production of 500kg. Manufacturing of all glass products took place in Cambridge, MA over four months. Each product was packaged individually with a protective case and palletized together before shipping to the exhibition site in Milan, Italy. Pre-cured dry joint interface and modular assembly system facilitated the construction process, completing the installation of all three glass columns in a few days. A programmable high intensity LED system with motion control system was installed inside each glass column. Each layer of the printed glass acted as an optical lens, and as the LED system traveled up and down inside the column. Interplay between the traveling light and the gradient morphology of the glass wall was optically magnified, transforming the entire exhibition space into a dynamic kaleidoscope of luminous caustics.

Figure 4: Installation of the glass columns at the Milan Design Week 2017, overall view of the three columns with integrated lighting system (left), and close-up view of the caustics on the floor (right)

4. Characterization

In parallel with production of the glass columns, a series of laboratory tests was conducted to characterize the mechanical responses of the printed glass. The products have distinct corrugation patterns along each layer, and two bending tests at different orientations with respect to the corrugations were conducted to evaluate flexural response and ultimate tensile strength. Compressive loading tests were conducted on two different scales to identify compressive strength of the glass itself as well as to evaluate compressive behavior of the full-scale glass products used in the assembly of the glass columns.

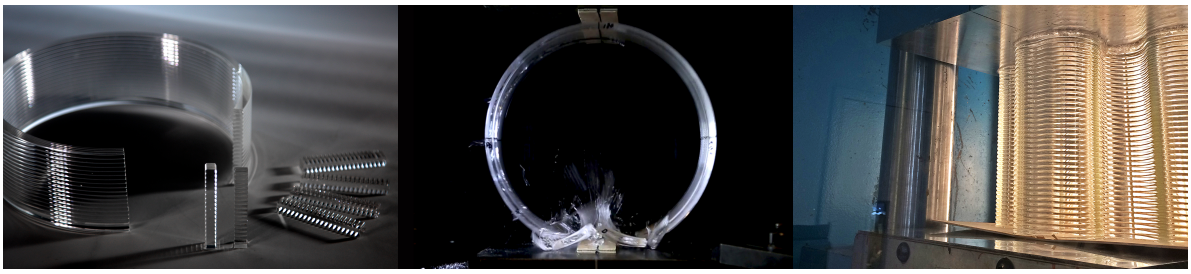

Figure 5: Laboratory tests on the glass products: rectangular bar samples for small-scale tests prepared from the cylindrical prints (left), full-scale bending test along the corrugation of the printed layers (middle), and full-scale compression test on a component used for one of the glass columns (right)

4.1. Tensile Strength

Flexure strength parallel to the corrugation of printed layers was measured by conducting a set of three-point bending tests on rectangular bar samples prepared from the larger prints. Samples were ground flat and polished to minimize influence of the mechanical flaws on exterior faces. Nominal dimensions of the rectangular bar samples were length 100 mm, width 13 mm, and effective thickness 9 mm. Samples were loaded in an orientation such that corrugations faced up and down. Flexure strength orthogonal to the corrugation of printed layers was examined by conducting a set of two-point bending tests on cylindrical prints. Nominal dimensions of the cylindrical samples were diameter 300 mm, height 100 mm and effective thickness 9 mm. Samples were loaded in an orientation such that the polished ends of the cylinders faced front and rear as shown in Figure 5. Four samples were tested for the three-point bending test, and two samples were tested for the two-point bending test. Table 2 reports the average values and their ranges from each test, where each symbol denotes peak load P, peak displacement δ, peak stress σ, and elastic modulus E.

Table 2: Summary of the flexure tests on rectangular bar samples and ring beam samples.

Test	*Sample*	*Value*	*P [kN]*	*δ [mm]*	*σ [MPa]*	*E [GPa]*
Three-Point	*Rect. Bar*	*Average*	*0.36±0.13*	*0.05±0.03*	*41±15*	*71±9*
Two-Point	*Ring Beam*	*Average*	*1.46±0.22*	*1.7±0.0*	*51±4*	*69± 4*

4.2. Compressive Strength

Small-scale compressive loading tests were conducted on a set of rectangular samples prepared from the larger prints. Nominal dimensions of the samples were 40 mm in height, 13 mm in width, and effective thickness of 9 mm. Samples were loaded in an orientation such that corrugations faced sideways. Full-scale compressive loading tests, as shown in Figure 5, were conducted on a set of glass products used for the columns. Nominal bounding dimensions of the products were 300 mm in diameter, 200 mm in height, and 9 mm in effective wall thickness. Four samples were tested at small-scale, and two samples were tested at full-scale. Table 3 reports the average values and their ranges from each test, denoted as peak load P, peak displacement δ, effective peak compressive stress σ_c, and elastic modulus E. The effective peak compressive stresses are reported based on the assumptions that samples were loaded in pure compression. The influences on the boundary conditions, resulting out-of-plane bending moment, and compound stresses at the perimeters are discussed in the later section on the numerical analysis.

Table 3: Summary of the compression tests on rectangular bar samples and column section samples.

Test	*Sample*	*Value*	*P [kN]*	*δ [mm]*	*σ_c [MPa]*	*E [GPa]*
Small-Scale	*Rect. Bar*	*Average*	*27.70±2.06*	*0.15±0.01*	*254±23*	*70±9*
Full-Scale	*Col. Parts*	*Average*	*1,620±47*	*0.41±0.0*	*147±18*	*72± 9*

4.3. Numerical Analysis

Average compressive strength of the full-scale glass column parts in the laboratory tests were significantly lower than the results from the small-scale samples. Influences on the boundary conditions and potential out-of-plane bending were believed to have played a role in lowering the overall compressive strength of the column parts. A series of numerical analyses were conducted to further examine the compressive behavior of cylindrical glass shells. Analysis was conducted using finite element analysis software Abaqus (Dassault Systèmes, Vélizy-Villacoublay, France). In order to simplify the geometrical influence, a standard cylindrical geometry was used for the numerical analysis with the dimensions of 300 mm in diameter, 200 mm in height, and 10 mm in thickness. The cylinder was meshed using three-dimensional solid elements (C3D8R) with effective resolution of three elements across the thickness, resulting in a mesh composed of 100 units in diameter, 67 units in height, and 3 units in thickness. Material properties were assigned as follows: elastic modulus of 70 GPa, density of 2,500 kg/m^3, and Poisson's ratio of 0.23. Linear elastic analysis was conducted with a load case defined as a constant rate of displacement assigned to the top face of the cylinder to simulate the laboratory compression test. Displacement rate was determined according to the stable time increment based on the given mesh size as approximately 4.6E-4 seconds [12]. Maximum displacement was set to 4 mm, and the simulation was run over 100 time increments noted as t_{total}. Two different boundary cases were studied to evaluate the influence of the in-plane friction at the top and bottom boundary faces and resulting out-of-plane bending moment to the effective axial stresses at the boundaries. In order to evaluate the results with respect to the material failure, critical stress values were determined based on the laboratory test results as 250 MPa in compression and 45 MPa in tension. While compressive strength of glass varies widely due to the inevitable influence of tensile stresses, this result was in agreement with the experimental values for soda-lime glasses reported in literature [13][14]. Table 4 reports the axial load and other values at the nearest time step instance when the internal principle stresses reached the critical value either in compression or tension. Each value is denoted as time step t, displacement δ, axial load P, effective compressive stress σ_c, compressive stress at the exterior edge of the boundaries ${}_{ext}\sigma_c$, and the interior edge of the boundaries ${}_{int}\sigma_c$, as well as the maximum principle tensile stress σ_t, and maximum shear stress τ. The effective compressive stress σ_c was evaluated by dividing the axial load by the cross-section area to serve as a comparison against the values reported in the Table 3. Rigid boundary conditions simulating maximum friction at the boundaries presents additional compressive stress due to the out-of-plane bending moment and subsequently lowers the maximum loading capacity of the glass cylinder under axial compression. These results demonstrate the significant influence of the boundary condition on the structural capacity of the test geometry, resulting in a 22 % difference in compressive strength. Further analyses are being conducted to address the implications of the geometrical simplifications and other factors that may account for the remaining differences found in the laboratory tests.

Table 4: Summary of the numerical analysis of the thick-wall cylinders.

Boundary	t/t_{total}	δ	P	σ_c	${}_{ext}\sigma_c$	${}_{int}\sigma_c$	σ_t	τ
	[step]/[step]	*[mm]*	*[kN]*	*[MPa]*	*[MPa]*	*[MPa]*	*[MPa]*	*[MPa]*
Rigid	*13.9/100.0*	*0.556*	*1,868*	*198.2*	*251.1*	*152.5*	*4.4*	*22.1*
Roller	*21.0/100.0*	*0.828*	*2,221*	*235.7*	*250.4*	*250.4*	*3.6*	*3.4*

5. Conclusion

This paper reports the novel design, engineering, and construction of large-scale 3D printed glass structures enabled by the development of a new high-fidelity large-scale additive manufacturing technology for optically transparent glass. The resulting structures, manifested in the form of three-meter tall freestanding glass columns, were optimized under material constraints of viscoelastic filaments to provide highly efficient structural and optical performance. A series of material and mechanical characterizations were conducted to evaluate the fidelity and repeatability of the new manufacturing platform and the structural performance of the resulting glass products in order to determine the safety factors required to execute the public installation. The 3D printed glass structures

presented here were exhibited for the first time at the Triennale Design Museum as part of the Milan Design Week 2017. The G3DP2 technology transforms the way glass is made, forging a path to unique glass architecture in which an ancient material can now be controlled with modern digital design. Future work investigating the complex relationship between manufacturing process, geometry, and structural performance will be critical to the deployment of 3D printed glass in our skylines.

6. Acknowledgement

The authors would like to thank Mori Building Co. Ltd, for their initial support and funding for the development of the G3DP2 platform, LEXUS for their support in hosting the first architectural installation of the 3D printed glass structures, as well as GETTYLAB for their continued support. We would like to thank Andrew Magdanz, Susan Shapiro, Mary Ann Babula, DJ Benyosef, and Robert Phillips of Almost Perfect Glass for hosting the team and providing supports and insights in glass making. We thank Spiral Arts Inc., Nikon USA, Smart Ceramics, Skutt Kilns, Teknic Inc., THK, Bell-Everman, Deltech Furnaces, Engineered Ceramics, the MIT Central Machine Shop, and Simpson Gumpertz & Heger for their technical support and collaborative development of the glass printing technology. We thank Front Inc. and Pentagram for additional contributions to the installation, and La Triennale di Milano for hosting our exhibition. We thank the MIT Media Lab and the MIT Center for Bits and Atoms for use of their facilities, and The Mediated Matter Group for their continuing teamwork and support for the project.

7. Disclosure

Authors C. Inamura, M. Stern, D. Lizardo, P. Houk, and N. Oxman are listed inventors on patent application US15331898, "Methods and Apparatus for Additive Manufacturing with Molten Glass."

8. Reference

[1] S. C. Rasmussen, *How Glass Changed the World*. Springer, 2012.
[2] B. Addis, "The Crystal Palace and Its Place in Structural History," *Int. J. Sp. Struct.*, vol. 21, no. 1, pp. 3–19, 2006.
[3] S. Douglas, R. W., Frank, *A History of Glassmaking*. London and Tonbridge: The Whitefriars Press Ltd., 1972.
[4] N. Wintour, "The glass industry : Recent trends and changes in working conditions and employment relations," 2015.
[5] J. Klein *et al.*, "Additive Manufacturing of Optically Transparent Glass," *3D Print. Addit. Manuf.*, vol. 2, no. 3, pp. 92–105, 2015.
[6] C. Inamura, "Towards a New Transparency: High Fidelity Additive Manufacturing of Transparent Glass Structures across Scales," Massachusetts Institute of Technology, 2017.
[7] F. Kotz *et al.*, "Three-dimensional printing of transparent fused silica glass," *Nature*, vol. 544, no. 7650, pp. 337–339, 2017.
[8] Today Prototype, "Micron3DP Announces Improved Glass 3D Printer," 2017. [Online]. Available: http://www.prototypetoday.com/micron3dp/micron3dp-announces-improved-glass-3d-printer. [Accessed: 01-Jan-2017].
[9] T. Gutowski *et al.*, "Note on the Rate and Energy Efficiency Limits for Additive Manufacturing," *J. Ind. Ecol.*, vol. 21, pp. S69–S79, 2017.
[10] C. Bedon and C. Louter, "Finite Element analysis of post-tensioned SG-laminated glass beams with adhesively bonded steel tendons," *Compos. Struct.*, vol. 167, pp. 238–250, 2017.
[11] S. R. Ledbetter, A. R. Walker, and A. P. Keiller, *Structural Use of Glass*, vol. 12, no. September. 2006.
[12] J. Pelfrene, S. Van Dam, R. Sevenois, F. Gilabert, and W. Van Paepegem, "Fracture Simulation of Structural Glass by Element Deletion in Explicit FEM," *Challenging Glas. 5 Conf. Archit. Struct. Appl. Glas.*, no. June, pp. 439–454, 2016.
[13] F. Oikonomopoulou, F. Veer, R. Nijsse, and K. Baardolf, "A completely transparent, adhesively bonded soda-lime glass block masonry system," *J. Facade Des. Eng.*, vol. 2, no. 3–4, pp. 201–221, 2015.
[14] J. Pedro, F. Olim, P. Sandra, S. Jordão, and E. C. Louter, "Structural Behaviour of Post-Tensioned Glass Beams Structural Behaviour of Post-Tensioned Glass Beams Dissertation submitted for the degree of Master of Civil Engineering Specialization in," 2014.